UDC 532.592
DOI https://doi.org/10.26661/2413-6549-2021-1-03

NUMERICAL SIMULATION OF A SOLITARY WAVE INTERACTION WITH SUBMERGED OBSTACLES

Gorban I. M.
PhD, Senior Research Fellow,
Senior Research Fellow at the Department of Technical Hydromechanics
Institute of Hydromechanics of the National Academy of Sciences of Ukraine
Marii Kapnist str., 8/4, Kyiv, Ukraine
orcid.org/0000-0001-9662-2813
ivgorban@gmail.com

Korolova A. S.
PhD,
Senior Research Fellow at the Department of Technical Hydromechanics
Institute of Hydromechanics of the National Academy of Sciences of Ukraine
Marii Kapnist str., 8/4, Kyiv, Ukraine
orcid.org/0000-0003-0693-4552
kan5nas@gmail.com

Key words: *wave propagation, free surface, wave-structure interactions, vortex field, vertical barrier, method of boundary integral equations, vortex method.*

The propagation of a solitary wave over a submerged obstacle installed at the channel bottom is numerically investigated. The topic is closely related to the operation of protective structures in natural bodies of water used for dissipation of wave energy. The developed numerical technique couples the method of boundary integral equations used to determine the free surface deformations and the vortex scheme for modeling the vortex field generated by the wave. In order to examine the validity of the model, the calculated free surface elevations were compared for a special case with corresponding data of the experimental research conducted in the hydrodynamic flume of the Institute of Hydromechanics. The comparison has been demonstrated that the present numerical scheme provides a good estimate as of reflected as of transmitted waves, which form above a submerged obstacle. Systematic calculations of the propagation of a solitary wave over submerged vertical barriers of different heights and lengths are performed. Their results point out that the type of interaction of a solitary wave with a barrier depends on the coefficient, which is the ratio of the incident wave amplitude to the thickness of the water column over the obstacle. When its value is less than the critical value, which is about 1, the incident wave splits smoothly into reflected and transmitted solitons and it breaks down otherwise causing chaotic oscillations of the free surface. The detail investigation of the vortex flow generated by the solitary wave near a vertical barrier detected two large-scale opposite vortices forming one after another at the obstacle tip. Interacting with the obstacle and channel bottom, the vortices grow to the size of the water depth and are shed to the flow in both the upstream and downstream directions. The vortices specify generation of water flows and intensity of turbulent processes near the obstacle. It is revealed that the influence of the vortex field on the stability of the submerged obstacle depends on its height. When the barrier is tall, the vortices go up to the free surface and are carried away by the collinear flow. In the case of a low obstacle, the vortex flow dissipates in its vicinity causing bottom erosion in this region.

ЧИСЕЛЬНЕ МОДЕЛЮВАННЯ ВЗАЄМОДІЇ СОЛІТОННОЇ ХВИЛІ ІЗ ЗАНУРЕНИМИ ПЕРЕШКОДАМИ

Горбань І. М.
кандидат фізико-математичних наук, старший науковий співробітник,
старший науковий співробітник відділу технічної гідромеханіки
Інститут гідромеханіки Національної академії наук України
вул. Марії Капніст, 8/4, Київ, Україна
orcid.org/0000-0001-9662-2813
ivgorban@gmail.com

Корольова А. С.
кандидат фізико-математичних наук,
старший науковий співробітник відділу технічної гідромеханіки
Інститут гідромеханіки Національної академії наук України
вул. Марії Капніст, 8/4, Київ, Україна
orcid.org/0000-0003-0693-4552
kan5nas@gmail.com

Ключові слова: *поширення хвилі, вільна поверхня, взаємодія хвилі з конструкцією, вихрове поле, вертикальний бар'єр, метод граничних інтегральних рівнянь, вихровий метод*

Чисельно досліджується поширення солітонної хвилі в каналі, на дні якого встановлено занурену перешкоду. Ця проблема тісно пов'язана з експлуатацією захисних споруд для розсіювання енергії хвиль у природних водоймах. Розвинена модель поєднує метод граничних інтегральних рівнянь, що застосовується для визначення деформацій вільної поверхні, і вихрову схему для розрахунку вихрового поля, яке генерується хвилею. Для її валідації залучені дані аналогічних експериментальних досліджень, що проводилися в гідравлічному лотку Інституту гідромеханіки. Збіг експериментальних та чисельних результатів щодо еволюції вільної поверхні вказує на те, що запропонована теоретична модель адекватно описує параметри як прохідної, так і відбитої хвиль, які утворюються над зануреною перешкодою. Виконані розрахунки поширення солітонної хвилі над зануреними вертикальними бар'єрами різної висоти та довжини. З їхніх результатів випливає, що тип взаємодії солітонної хвилі з бар'єром залежить від коефіцієнту, який є відношенням амплітуди падаючої хвилі до товщини стовпа води над перешкодою. Коли його значення менше за критичне, яке становить приблизно 1, падаюча хвиля м'яко поділяється на відбитий та прохідний солітони. В іншому разі вона руйнується, що викликає хаотичні коливання вільної поверхні. Детальне дослідження вихрової течії, яка генерується солітонною хвилею поблизу бар'єру, виявило в цій області два великих протилежно спрямованих вихори, що послідовно утворюються на вершині бар'єру. Взаємодіючи з перешкодою та дном каналу, вони зростають до розмірів, співставних з глибиною води, та відриваються. Один із них рухається за течією, інший – проти неї. Ці вихори визначають розвиток течій та інтенсивність турбулентних процесів поблизу перешкоди. Отримано, що вплив вихрового поля на стійкість зануреної конструкції залежить від її висоти. Коли бар'єр високий, вихори піднімаються і зносяться супутньою течією. У разі низької перешкоди вихровий потік дисипує поблизу неї, спричиняючи ерозію дна в цій області.

Introduction. The interaction of surface waves with submerged obstacles in shallow water is a classic problem of coastal and marine hydrodynamics. The topic is closely related to the construction of submerged protective structures dissipating wave energy and preventing coastal erosion. Besides, it deals with natural factors that may lead to dangerous processes in coastal zones such as the wave propagation over coral reefs or continental shelf. The importance of the problem has led to a large number of theoretical and experimental studies over the past decades. In most of them, a solitary wave is considered owing to unique relationship between wave nonlinearity and steepness that reduces the number of important parameters to one [1]. Solitary waves present a limiting condition for the run-up of an extreme non-linear long wave, such as tsunami [2]. Besides, the connection of the solitary solution with ocean waves is ensured by the fact that periodic waves in deep water are unstable and break up into groups whose circumferential line has the properties of a soliton [3].

Earlier researches were based on the solitary wave theories in the shallow water such as Boussinesq and the KdV equations [4; 5]. The models predict accurately the reflected and transmitted waves within of its applicability but calculate higher wave amplitudes as compared with experimental data for strongly non-linear problems [5; 6]. To overcome this restriction, the Boundary Element Method (BEM) was applied. The BEM is based on the potential flow theory and adapted to solve the Laplace equation with nonlinear boundary conditions on the free surface. Using this approach, Grilli et al. [7] described the wave breaking above obstacles of different shape. The influence of wave amplitude and obstacle parameters on wave behavior was described in [7], where the BEM was applied for studying the interaction of a solitary wave with a submerged semicircular cylinder. One of the latest applications of the potential theory to calculation of wave evolution is simulation of the interaction of a solitary wave with a wave energy converter in the presence of bottom irregularities and collinear currents [9].

It is well known that the solitary wave passing over a submerged obstacle causes intense vortical flows inside the water column which strongly affect the wave energy and stress distribution on the bed. The potential theory with irrotational flow assumption is not suitable to investigate the flow separation and generation of vortex field near the structure. To take into account the above- mentioned effects, the numerical methods based on the viscous flow equations were developed. The volume of fluid (VOF) and mark-and-cell chart (MAC) methods are two main approaches for modeling viscous fluid flows with strong nonlinearity on a free surface. Those employ the Reynolds Averaged Navier–Stokes (RANS) equations with a $k-\varepsilon$ non-linear turbulence closure model [10]. Basing on these approaches, significant advances have been made in understanding the phenomena accompanying the interaction of a solitary wave with submerged obstacles [11; 12; 13].

The great disadvantages of the grid-based numerical schemes are the difficulty in tracking the fluid interface and implementation of the free surface boundary conditions, especially when a moving grid is used. An alternate approach is using the Lagrangian-type numerical schemes which model a free surface by a system of singularities moving with the fluid particles. It allows reducing the initial boundary value problem of determining the free surface configuration to a system of the integral equations in respect to the strength of singularities [14]. In this approach, the generation of vorticity by the free surface is predominantly neglected, which greatly simplifies the boundary conditions. One can find examples of the use of the Lagrangian scheme in papers [15; 16], where interaction of a solitary wave with a submerged rectangular structure is considered. Note the viscous flow under the free surface is calculated with the vortex method, which is based on the velocity-vorticity form of the Navier-Stokes equations. The vortex field is shown to be the main factor determining the drag of the structure.

A similar theoretical model is developed in the present study. Its difference from the previous schemes lies in the simpler involvement of the free surface dynamic condition, which, nevertheless, does not affect the calculation results. Taking into account that the generation of vorticity at the free surface is ignored, the vortex scheme developed by authors in paper [17] can be utilized for viscous simulation. The validity and efficiency of this algorithm has been confirmed when solving various two-dimensional problems of viscous fluid dynamics [18; 19; 20]. In order to verify the mathematical model, a set of laboratory experiments in the hydrodynamic flume was performed with a solitary wave passing above a vertical barrier. In both the numerical simulation and experiment, the free surface elevations were measured in the given locations and the obtained results were compared. A good match between the data of the calculations and the physical experiment was obtained as for reflected as for transmitted wave.

Problem statement. A solitary wave travelling in viscous incompressible fluid over a submerged rectangular obstacle of height d and length a is considered (Fig. 1). A Cartesian coordinate system is fixed such that its origin is connected with the midpoint of the obstacle, the x-axis lies in the bottom and the y-axis points vertically upward. The still water depth is h and the amplitude of the incident wave is A_i. Taking into account that the fluid in the flume is under the action of gravity, its motion is governed by the

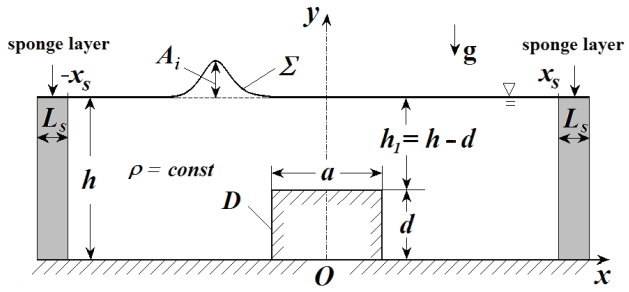

Fig. 1. Schematic diagram of the numerical flume with a solitary wave passing over a submerged rectangular obstacle

following system of equations:

$$\nabla \cdot \vec{V} = 0\,, \tag{1}$$

$$\frac{\partial \vec{V}}{\partial t} + \left(\vec{V}\cdot\nabla\right)\vec{V} = -\nabla P + \frac{1}{\mathrm{Re}}\nabla^2\vec{V}\,, \tag{2}$$

where the hydrodynamic pressure P is equal to the total pressure p minus the hydrostatic pressure: $P = p + y/Fr^2$, $\vec{V}$ is the velocity and t is the time. The variables in (1), (2) are scaled by the still water depth h and the phase speed of linear long-wave $\sqrt{gh}$, where g is the acceleration due to the gravity; $\bar{t} = t\sqrt{gh}/h = t\sqrt{g/h}$ is the dimensionless time (the overline in (2) and further is omitted). The Reynolds number is evaluated based on the depth-averaged velocity under the wave crest $U = \frac{A_i}{h}c$, where $c = \sqrt{g(h+A_i)}$ is the wave celerity, then $\mathrm{Re} = Uh/\nu = A_i\sqrt{g(h+A_i)}/\nu$. The Froude number is introduced as $Fr = c/\sqrt{gh}$.

The kinematics boundary condition at the free surface Σ forces the surface to follow the trajectories of the fluid particles z_Σ lying on it. This means that the following evolutionary equation is realized:

$$\frac{dz_\Sigma}{dt} = \vec{V}_\Sigma\,. \tag{3}$$

The dynamic condition declares the continuity of stresses when jumping across a free surface. It is written under the assumption that the surface tension and viscosity are neglected:

$$p_\Sigma = p_a\,, \tag{4}$$

where p_a denotes the atmosphere pressure.

The non-leaking and no-slip boundary conditions must be required at the bottom:

$$\vec{V}(\vec{r}_b,t)\cdot\vec{n} = 0\,, \tag{5}$$

$$\vec{V}(\vec{r}_b,t)\cdot\vec{\tau} = 0\,, \tag{6}$$

where $\vec{r}_b$ denotes the radius-vector of bottom points, $\vec{n}, \vec{\tau}$ are the normal and tangential unit vector on the bottom, respectively.

To avoid the wave reflection at the lateral boundaries of the numerical wave flume, wave damping is introduced following the method proposed in [14]. For this reason, numerical sponge layers are put at both lateral boundaries to absorb the outward-traveling waves.

Numerical model. Boundary value problem (1)-(6) is solved using the numerical model that combines the boundary integral equation method calculating the free surface evolution and the vortex scheme for simulation of the viscous flow near an obstacle. It has been described in details in papers [17; 18] therefore generalities of the model are only considered here.

Since the vorticity generation at the free surface is ignored, the flow is irrotational far from the submerged structure. At the same time, the wave motion causes an intense vortical flow in close proximity to the structure. Following the Helmholtz decomposition principle [21], the flow under consideration is decomposed into the potential part in the thin layer near the free surface and the rotational part everywhere except the fluid boundary. Then the velocity field is represented by the sum:

$$\vec{V}(\vec{r},t) = \nabla\phi + \nabla\times(\Phi\vec{k})\,, \tag{7}$$

where $\vec{r}$ denotes the radius-vector of a point, ϕ and $\Phi\vec{k}$ are the scalar and vector potential of the irrotational and vortical flows, $\vec{k}$ is the unit vector out of the page.

In the present model, the vortex flow is described by the function of vorticity $\omega = \vec{k}\cdot\nabla\times\vec{V}$. To take into account the free surface and bottom irregularity, the method of boundary integral equations is applied. According to this approach, the free surface and the underwater obstacle boundary are modeled by vortex distributions of strength μ and γ respectively [14; 17]. According to these assumptions, velocity field (7) is written by the following equation:

$$\begin{aligned}\vec{V}(\vec{r},t) \;=\; & \nabla\int_\Sigma \mu(\vec{r}',t)\,\frac{\partial G(\vec{r},\vec{r}')}{\partial\vec{n}}\,dl(\vec{r}') \;+\\ & +\nabla\int_D \gamma(\vec{r}',t)\,\frac{\partial G(\vec{r},\vec{r}')}{\partial\vec{n}}\,dl(\vec{r}') \;+\\ & +\int_S \omega(\vec{r}',t)\vec{k}\times\nabla G(\vec{r},\vec{r}')\,ds(\vec{r}')\,,\end{aligned} \tag{8}$$

where Σ, D denote the free surface and the boundary of obstacle respectively, S is the viscous flow domain, $G(\vec{r},\vec{r}')$ is the Green function for a point vortex in the half-plane [21].

For convenience, we describe the flow field with a complex coordinate $z = x + iy$. The free surface Σ and obstacle boundary D are parameterized in terms of linear parameters e and s respectively, which are the Lagrangian coordinates of the points lying on these interfaces. The vorticity field ω is approximated by a set of vorticity carrying particles as proposed in [22]:

$$\omega(z,t) \approx \sum_{j=1}^{N}\Gamma_j^*(t)\,f_\delta(z-z_j)\,, \tag{9}$$

where Γ_j^* and z_j are the circulation and coordinate of the $j-$th vortex, N is the number of free vortices, f_δ is the distribution function of vortex.

Within this approach, equation (8) can be rewritten as:

$$\vec{V}(z,t)=\frac{1}{2\pi i}\int_\Sigma \mu(e',t)\left[\frac{1}{z-z(e',t)}-\frac{1}{z-z^*(e',t)}\right]de'+$$
$$\frac{1}{2\pi i}\int_D \gamma(s',t)\left[\frac{1}{z-z(s')}-\frac{1}{z-z^*(s')}\right]ds'$$
$$+\frac{1}{2\pi i}\sum_{j=1}^{N}\Gamma_j^*\left[\frac{1}{z-z_j(t)}-\frac{1}{z-z_j^*(t)}\right], \qquad (10)$$

where the asterisk denotes conjugation about the *Ox*-axis. Note the principal value of the integrals is considered in (10) in order to avoid singularities.

In the discrete scheme, the continuous vortex sheets located along Σ and D are replaced by sets of the panels of length Δe and Δs. Complex coordinates of the panels are:

$$(z_\Sigma)_m(t)=z_\Sigma(e_m,t),\ (z_D)_k=z_D(s_k), \qquad (11)$$

where $m=1,2,...,N_\Sigma$, $k=1,2,...,N_D$, N_Σ, N_D are the numbers of the panels. The strengths $\mu(s,t)$ and $\gamma(s,t)$ are assumed to be constant along a panel, so we deal with distributions of the piecewise continuous functions:

$$\mu_m(t)=\mu(e_m,t),\ \gamma_k(t)=\gamma(s_k,t). \qquad (12)$$

To determine these functions, free surface dynamic condition (4) and non-leaking condition (5) are applied in accordance with the technique developed in [23]. It involves solving the evolutionary equations for $(z_\Sigma)_m$ and ϕ_m. The first of them is kinematic condition (3), and the second follows from dynamic condition (4). Then the system of linear algebraic equations with respect to $\mu_m(t)$ and $\gamma_k(t)$ is solved. One can find a detailed description of this method in paper [18].

Following [10], we utilize a fourth-order Adams–Bashforth–Moulton (ABM) predictor-corrector scheme to integrate the evolutionary equations for $(z_\Sigma)_m$ and ϕ_m. The regularization procedure is fulfilled in the end of a time step to eliminate numerical instabilities on the computed free surface. According to this procedure, the panel lengths are recalculated so that all segments should be equal. Additionally, the strength function $\mu_m(t)$ is changed on the m-th panel proportionally to the new value of Δe. Note that the number of panels at the free surface does not change during the entire modeling process. This regularization improves considerably the stability of free-surface computations that allows extending the range of parameters of the problem under consideration at which the simulation will be successful. In particular, breaking solitary waves are considered together with regular processes.

Wave reflection on side walls of the numerical flume is eliminated with the help of the sponge layers damping perturbations of the scheme parameters. This way involves the incorporation of additional damping terms into the evolutionary equations as for points $(z_\Sigma)_m$ as for potential ϕ_m. For the first time, the technique was proposed in [24] and since then it has been successfully used when integrating the problems with a free-surface [11; 13].

In this study, modeling the evolution of a solitary wave when it passes over a submerged obstacle is coupled with calculations of the vorticity field generated by the wave. The last are performed with the well-known vortex method [22], which applies the velocity–vorticity form of the Navier–Stokes equations instead the traditional pressure–velocity formulation. If one takes the curl of the Navier–Stokes equations, the pressure field will be eliminated including the component associated with gravity. Taking into account that the generation of vorticity at the free surface is neglected, the vortex scheme developed by us in paper [17] can be utilized for viscous simulation. The validity and efficiency of this algorithm has been confirmed when solving various two-dimensional problems of viscous fluid dynamics [18; 19; 20].

Model verification. The developed numerical model has applied by us for simulation of solitary wave propagation over a step [18]. Comparison of the obtained results with the experimental data from paper [25] shown that the simulation predicted accurately the fission process with respect the dependence of the number of secondary solitons on the incident wave amplitude and step height.

In this study, the model's ability to simulate accurately the evolution of a free surface is verified against laboratory experiments with a solitary wave passing over a submerged vertical thin barrier. The experiments were conducted in a glass-wall flume of the Institute of Hydromechanics. The laboratory setup, equipment and experimental technique have been described in detail in paper [26]. Fig. 2 illustrates the normalized parameters of the problem under consideration as well as positions of the gauges utilized to fix free surface elevations as in laboratory experiment as in numerical modeling.

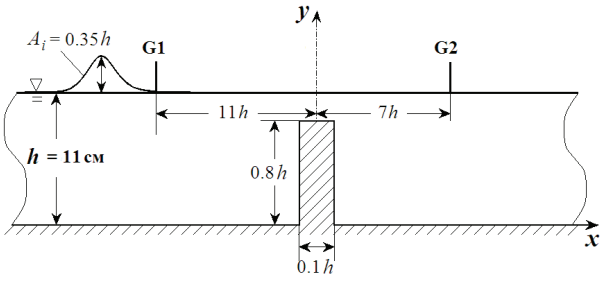

Fig. 2. Parameters of laboratory and numerical researches

Fig. 5 demonstrates the time histories of instantaneous free surface elevations $\eta(t)$ at the selected locations G1 and G2 derived in the measurements (solid black lines) and in the calculations (dotted red lines). The comparison indicates that the numerical calculations fit the measurements well for the main waveforms in terms of the incident and reflected waves recorded by the gauge G1 and the transmitted wave recorded by the gauge G2. It should also be noted that the experimental and numerical results are in good agreement with respect to the propagation rate of free surface perturbations. Here and below, the dimensionless time $t = 0$ is defined as the instant when the crest of a solitary wave passes exactly above the top of the obstacle.

Setup of the numerical experiment and results. A numerical wave flume used in this study is of 1m depth and 140m length. Normalized parameters of the problem will be further considered. The width of the absorbing layers adjoining the lateral sides of the flume is put to $2h$. The rectangular obstacle is situated in the middle of the computational domain. At the initial time instance, the wave crest is located at $x/h = -20$ and then it propagates from left to right. To derive the initial data for a solitary wave, profile and velocity potential, the MatLab implementation of the iterative method proposed in [27] is utilized. Since it computers the approximated solitary solution of the Euler equations, both horizontal and vertical motions of fluid particles under the wave can be considered. This allows modeling not only the free surface evolution but also the dynamics of the vortex field generated by a solitary wave. The number of vortex panels along the free surface is equal to $N_\Sigma = 2800$; a uniform grid system of $\Delta x = \Delta y = 0.01h$ is put on the flow field; the time step is $\Delta t = 0.005\sqrt{g/h}$; $\mathrm{Re} = 0.69 \cdot 10^6$.

Fig. 4 demonstrates the free surface elevations $\eta(x,t)$ arising when the solitary wave of amplitude $A_i/h = 0.2$ passes over submerged rectangular barriers of different height d/h and length a/h. The results represented in Figs. 4*a*,*b*,*c* are obtained at $a/h = 0.1$, so they reflect the wave evolution above a thin vertical barrier. It is reasonable to classify those involving the quantitative parameter $K_{\text{int}} = A_i/(h-d)$. It was introduced in [26] based on the data of laboratory experiments and was called the interaction coefficient. Fig. 4*a* illustrates the weak interaction of the solitary wave with the thin barrier of height $d/h = 0.7$. It is characterized by the growth of the incident wave over the obstacle and its smooth splitting into the reflected and transmitted solitons moving in opposite directions. Note that the interaction coefficient in this case is $K_{\text{int}} \approx 0.65$.

Free surface profiles in Fig. 4*b* are obtained at $d/h = 0.8$, which corresponds to the interaction coefficient $K_{\text{int}} \approx 1$. The transmitted wave has not yet destroyed here, but the dynamics of the process is complicated due to dispersion effects conditioned by the generation of a chain of secondary solitons. Note also that the local rising of the free surface level in Figs.4a, 4b observed immediately behind the obstacle is produced by the intense recirculation flow developed in this area.

Fig. 4c demonstrates the strong influence of a submerged barrier on the wave, which is characterized by the interaction coefficient $K_{\text{int}} \approx 2$ ($d/h = 0.9$). In this case, the incident wave is divided into three parts. The reflected and transmitted solitons moving in opposite directions are formed, as usual. In addition, a part of the water lying directly above the barrier first rises, and then falls sharply and collapses, as a result, chaotic pulsations of the free surface arise in this area. This process is characterized by large gradients of the free surface and the formation of water splashes. Finally, two regular secondary solitons separate from this region, which follow the transmitted wave. It is obvious the more complex the interaction of the wave with the obstacle the more wave energy is expended on secondary processes, which primarily

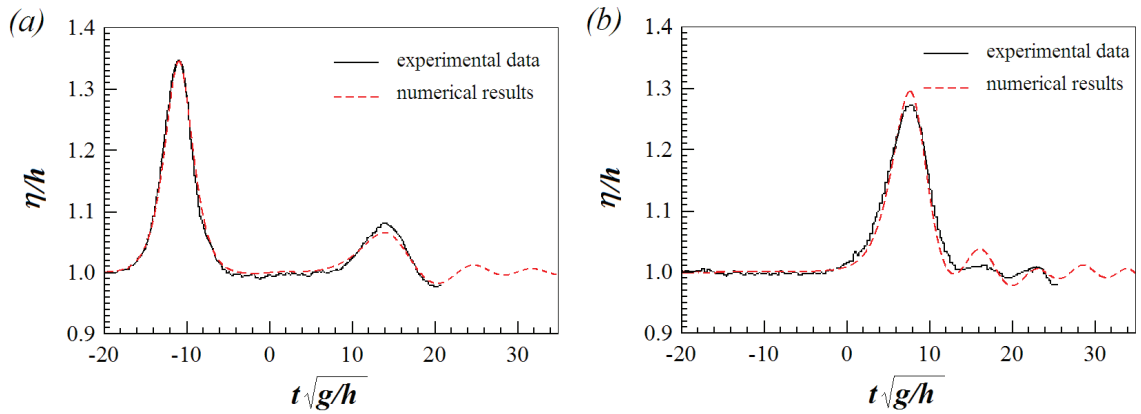

Fig. 3. Free surface elevations for the solitary wave interacting with a submerged barrier derived in experimental measurements and calculations by gauges G1 (left) and G2 (right)

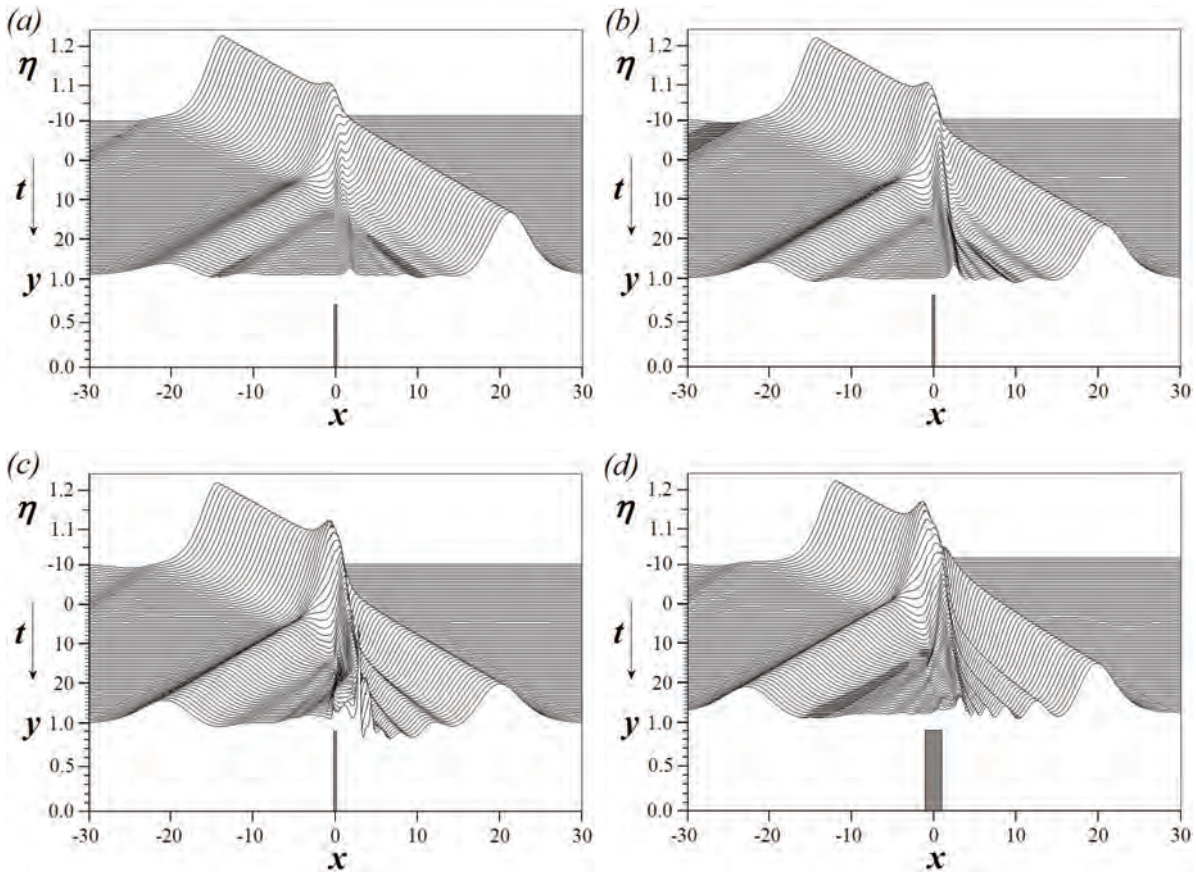

Fig. 4. Transformations of a solitary wave of amplitude $A_i / h = 0.2$ above a submerged rectangular structure:
(a) **–** $d / h = 0.7, a / h = 0.1$**,** ***(b)*** **–** $d / h = 0.8, a / h = 0.1$**,**
(c) **–** $d / h = 0.9, a / h = 0.1$**,** ***(d)*** **–** $d / h = 0.9, a / h = 1.5$

affects the characteristics of the transmitted soliton. One can see a significant decrease in the amplitude of the transmitted wave in Fig. 4*c* in comparison with the previous cases.

The calculation results also show that the wave destruction over long rectangular structures is not as intense as over thin ones, even if they are quite high. This conclusion is confirmed by the free surface profiles depicted in Fig. 4*d*, which are obtained when the solitary wave passes over the rectangle of height $d / h = 0.9$ and length $a / h = 1.5$. The abrupt change in water depth is seen to increase greatly the free surface nonlinearity. As a result, the incident wave grows above the obstacle and then it divides into a reflected soliton and a transmitted wave. In addition, the intense secondary solitons and dispersive wave chain are generated. At the same time, no destructive processes in the form of chaotic pulsations of the free surface near the structure are observed.

The wave propagation over a submerged obstacle is accompanied not only by effects on the free surface, but also by underwater processes. A travelling solitary wave generates the intense flow of liquid particles under the free surface. When this flow meets an obstacle, it has to rebuild in accordance with the obstacle configuration. Due to the flow narrowing, a shear layer is formed near the structure, followed by flow separation and the formation of large-scale vortices. Fig. 5 illustrates the velocity fields induced by the solitary wave of amplitude $A_i / h = 0.2$ around the submerged barriers of length $a / h = 0.1$ and height $d / h = 0.7$ (left) and $d / h = 0.9$ (right).

It is known [28], that the length L_s of a solitary wave is related to its amplitude by the ratio $L_s / h \approx 10\sqrt{h / A_i}$. Then one obtains $L_s / h \approx 22$ at $A_i / h = 0.2$. This means that the formation of the shear layer due to the approaching wave begins when the distance between the wave crest and the barrier is about $11h$, which corresponds to the dimensionless time $\bar{t} = t\sqrt{g / h} \approx -10$.

Figs. 5*a*, 5*f* show the process of converting the shear layer into a clockwise vortex, here $\bar{t} = -8$. The vortex originates in the front edge of the barrier and rotates in the direction of wave movement. As the wave crest approaches the obstacle, the vortex continues to grow in size as depicted in Figs. 5*b*, 5*g* at $\bar{t} = -2$. Figs. 5*c*, 5*h* correspond to the instant when the crest of the solitary wave is at the top of the bar-

rier ($\bar{t} = 0$). The horizontal flow velocity reaches its maximum value over the obstacle, so the main vortex sheds out and begins to dissipate rapidly.

When the wave has passed the obstacle, the translatory motion of fluid particles almost completely ceases, as a result, the vortex zone remains close to the obstacle and grows to the depth of the water (Figs. 5*d*, 5*i*). The zone interacts with the channel bottom and the rear edge of the barrier forcing generation of the boundary layer which thickens and forms the secondary counterclockwise vortex above the obstacle tip. In Figs. 5*d*, 5*i* ($\bar{t} = 8$), the counterclockwise vortex is still remains attached to the rear edge of the barrier but further it moves upward and upstream and sheds out (Figs. 5*e,* 5*j*). Subsequently, the primary and secondary vortices reach the free surface and cause it to bulge. It follows from the present results that the evolution of the vortex field forces the water to move upward at the rear edge of the obstacle as well as in the direction opposite to the wave motion.

The influence of the barrier height on the vortex field evolution can be seen by comparing the left and right columns of Fig. 5. With a lower barrier height (left column), the main vortex develops near the structure and remains there until complete dissipation. When the barrier is high (right column), the gap between its top and the free surface is narrowed that leads to increasing the fluid velocity here. So, the primary clockwise vortex is more intense in this case

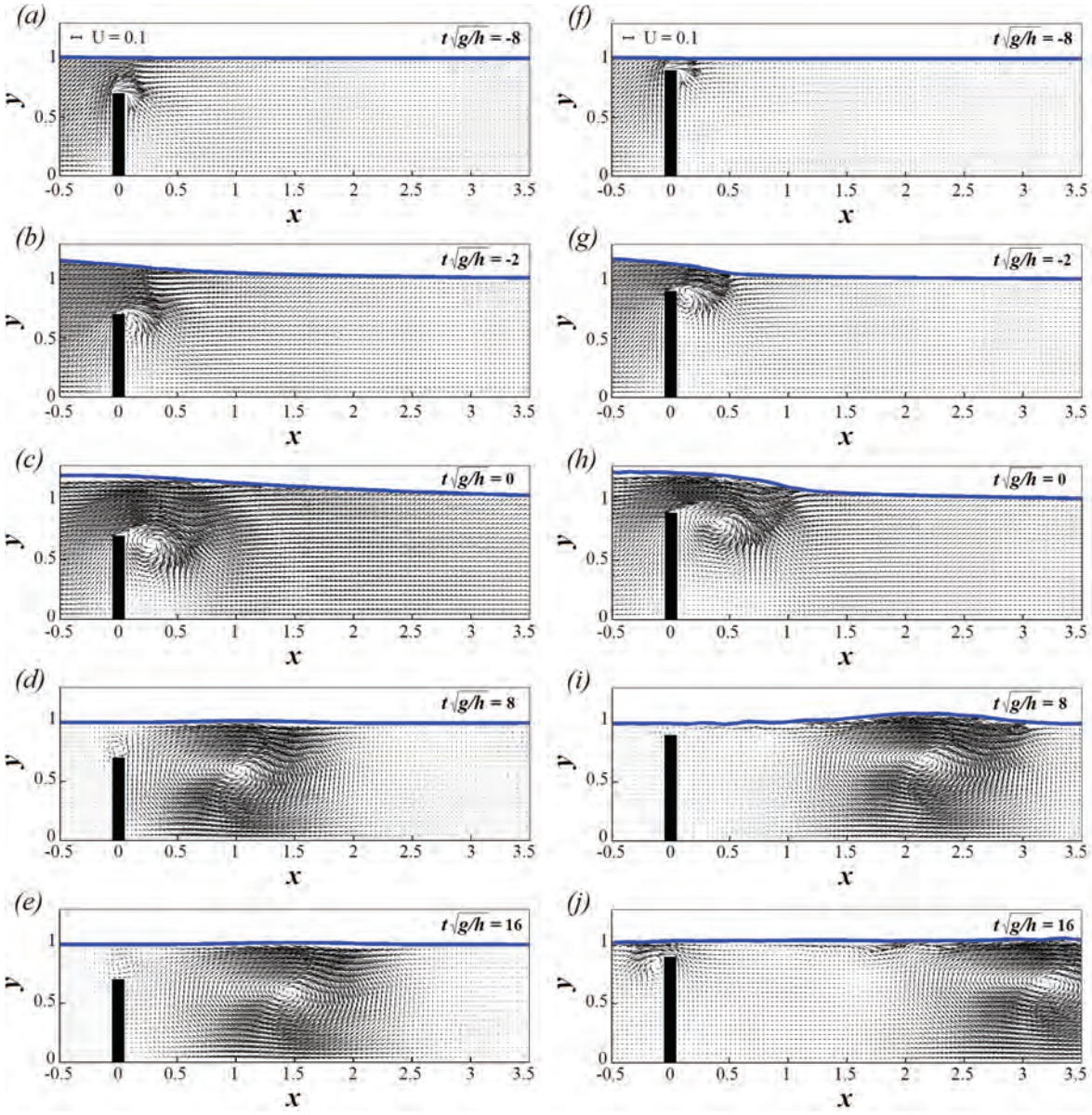

Fig. 5. Free surface elevations (blue) and velocity fields generated by a solitary wave of amplitude $A_i / h = 0.2$ around thin vertical barriers of height $d / h = 0.7$ (left) and $d / h = 0.9$ (right) at various time instants

and localizes closer to the free surface than to the bottom. It moves together with the transmitted soliton quickly leaving the region adjacent to the obstacle. Thus, the effect of a vortex flow on the channel bottom is stronger in the case of low obstacles located on the way of a solitary wave. At the same time, vortices generated behind high obstacles cause intense bulges of the free surface.

Conclusions. The numerical model for studying wave-structure interactions is presented. It combines the boundary integral method for description free-surface deformations and the vortex method for integrating the viscous fluid dynamic equations. The validity of this model is confirmed by the close match of the calculated elevations of the free surface for a special case with the corresponding data of experimental researches.

Two types of interaction of a solitary wave with a vertical barrier were revealed based on systematic calculations of the propagation of the solitary wave of normalized amplitude $A_i / h = 0.2$ over barriers of different heights. Those are the weak interaction, when the incident wave splits smoothly into the reflected and transmitted solitons, and strong interaction, when the wave breaks down. The scenario for the behavior of a solitary wave over a barrier depends on the interaction coefficient, which is the ratio of the amplitude of the wave to the thickness of the water column above the obstacle. It is obtained that the critical value of the interaction coefficient is about 1, at which the regimes change.

An analysis of the vortex fields created by the solitary wave around barriers of different heights shows that the fluid dynamics in the region is controlled by the interaction of two large opposite vortex structures generated at the barrier tip one after another. The effect of the vortex field on stability of the submerged structure depends on its height. When the barrier is tall, the vortices go up and are carried away by the collinear flow. In the case of a low obstacle, the vortex flow dissipates in its vicinity causing bottom erosion in this region.

BIBLIOGRAGHY

1. Miles J.W. (1980) Solitary waves. *Annual Review of Fluid Mechanics,* vol. 12, pp. 11–43. URL : https://doi.org/10.1146/annurev.fl.12.010180.000303.
2. Synolakis C. E. (1987) The run-up of solitary waves. *Journal of Fluid Mechanics,* vol. 185, pp. 523–545. URL : https://doi.org/10.1017/S002211208700329X.
3. Зейтунян Р.Х. (1995) Нелинейные длинные волны на поверхности воды и солитоны. *Успехи физических наук*, т. 165, № 12. С. 1403–1456.
4. Mei C.C., Black J.L. (1969) Scattering of surface waves by rectangular obstacles in waters of finite depth. *Journal of Fluid Mechanics*, vol. 38, no. 3, pp. 499–511. URL : https://doi.org/10.1017/S0022112069000309.
5. Seabra-Santos F. J., Renouard D. P., Temperville A. M. (1987) Numerical and experimental study of the transformation of a solitary wave over a shelf or isolated obstacle. *Journal of Fluid Mechanics*, vol. 176, pp. 117–134. URL : https://doi.org/10.1017/S0022112087000594.
6. Losada M.A., Vidal C., Medina R. (1989) Experimental study of the evolution of a solitary wave at an abrupt junction. *Journal of Geophysical Research*, vol. 94, pp. 557–566. URL : https://doi.org/10.1029/JC094iC10p14557.
7. Grilli S.T., Losada M.A., Martin F. (1994) Characteristics of solitary wave breaking induced by breakwaters. *Journal of Waterway, Port, Coastal and Ocean Engineering*, vol. 120, no. 1, pp. 75–92. URL : https://doi.org/10.1061/(ASCE)0733-950X(1994)120:1(74).
8. Cooker M.J., Vidal D.H., Dold J.W. (1990) The interaction between a solitary wave and a submerged semicircular cylinder. *Journal of Fluid Mechanics*, vol. 215, pp. 1–22. URL : https://doi.org/10.1017/S002211209000252X.
9. Cheng Li G., Ji C., Zhai G. (2020) Solitary wave slamming on an oscillating wave surge converter over varying topography in the presence of collinear currents. *Journal of Physics Fluids*, vol. 32, pp. 047102-1−047102-22. URL : https://doi.org/10.1063/5.0001402.
10. Lin P., Liu P.L.F. (1998) A numerical study of breaking waves in the surf zone. *Journal of Fluid Mechanics*, vol. 359, pp. 239–264. URL : https://doi.org/10.1017/S002211209700846X.
11. Chang K, Hsu T., Liu P. (2001) Vortex generation and evolution in water waves propagating over a submerged rectangular obstacle. *Journal of Coastal Enineering*, vol. 44, pp. 12–36. URL : https://doi.org/10.1016/S0378-3839(01)00019-9.
12. Huang C.-J., Dong C.-M. (2001) On the interaction of a solitary wave and a submerged dike. *Journal of Coastal Enineering*, vol. 43, pp. 265–286. URL : https://doi.org/10.1016/S0378-3839(01)00017-5.
13. Lin P.A. (2004) Numerical study of solitary wave interaction with rectangular obstacles. *Journal of Coastal Enineering*, vol. 51. pp. 35–51. URL : https://doi.org/10.1016/j.coastaleng.2003.11.005.
14. Baker G.R.,Meiron D., Orszag S.A. (1982) Generalized vortex methods for free-surface flow problems. *Journal of Fluid Mechanics*, vol. 123, pp. 477–501. URL : https://doi.org/10.1017/S0022112082003164.

15. Lin M.Y., Huang L.H. (2009) Study of water waves with submerged obstacles using a vortex method with Helmholtz decomposition. *Journal Numerical Methods in Fluids*, vol. 60. pp. 119–148. URL : https://doi.org/10.1002/fld.1873.
16. Lin M.Y., Huang L.H. (2010) Vortex shedding from a submerged rectangular obstacle attacked by a solitary wave. *Journal of Fluid Mechanics*, vol. 651, pp. 503–518. URL : https://doi.org/10.1017/S0022112010000145.
17. Горбань В.О., Горбань І.М. (2005) Вихрова структура потоку при обтіканні квадратної призми: числова модель та алгоритми управління. *Прикладна гідромеханіка*, т. 7, № 2. С. 8–26.
18. Gorban I.M. (2015) A numerical study of solitary wave interactions with a bottom step. *Continuous and Distributed Systems II. Springer, Cham*., vol. 30, pp. 369–387. URL : https://doi.org/10.1007/978-3-319-19075-4_22.
19. Gorban I.M., Khomenko O.V. (2016) Flow control near a square prism with the help of frontal flat plates. *Advances in Dynamical Systems and Control. Springer, Cham.*, vol. 69. pp. 327–350. URL : https://doi.org/10.1007/978-3-319-40673-2_17.
20. Basovsky V.G., Gorban I.M., Khomenko O.V. (2019) Modification of hydrodynamic and acoustic fields generated by a cavity with a fluid suction. *Modern Mathematics and Mechanics. Understanding Complex Systems. Springer, Cham*., pp. 137–158. URL : https://doi.org/10.1007/978-3-319-96755-4_9.
21. Lamb H. (1932) *Hydrodynamics*. London: Cambridge University Press.
22. Cottet G.-H., Koumoutsakos P. (2000) *Vortex methods: theory and practice*. London: Cambridge University Press.
23. Моляков Н.М. (1985) Нестационарное обтекание профиля у поверхности раздела жидкостей. *Труды ВВИа им. Жуковского*, т. 1313. С. 336–347.
24. Israeli M., Orszag S.A. (1981) Approximation of radiation boundary conditions. *Journal of Computer Physic*, vol. 41, pp. 115–135. URL : https://doi.org/10.1016/0021-9991(81)90082-6.
25. Seabra-Santos F. J., Renouard D. P., Temperville A. M. (1987) Numerical and experimental study of the transformation of a solitary wave over a shelf or isolated obstacle. *Journal of Fluid Mechanics*, vol. 176, pp. 117–134. URL : https://doi.org/10.1017/S0022112087000594.
26. Котельнікова А.С., Нікішов В.І., Срібнюк С.М. (2018) Експериментальне дослідження взаємодії поверхневої поодинокої хвилі з підводним уступом. *Гідродинаміка і акустика*. т. 1, № 1. С. 22−52. URL : https://doi.org/10.15407/jha2018.01.042.
27. Clamond D., Dutykh D. (2013) Fast accurate computation of the fully nonlinear solitary surface gravity waves. *Journal Computers & Fluids*, vol. 84, pp. 35–38. URL : https://doi.org/10.1016/j.compfluid.2013.05.010.
28. Madsen O.S., Mei C.C. (1970) The transformation of a solitary wave over an uneven bottom. *Journal of Fluid Mechanics*, vol. 39, № 4, pp. 781–791. URL : https://doi.org/10.1017/S0022112069002461.

REFERENCES

1. Miles J.W. (1980) Solitary waves. *Annual Review of Fluid Mechanics,* vol. 12, pp. 11–43. https://doi.org/10.1146/annurev.fl.12.010180.000303
2. Synolakis C. E. (1987) The run-up of solitary waves. *Journal of Fluid Mechanics,* vol. 185, pp. 523–545. https://doi.org/10.1017/S002211208700329X
3. Zeytunyan R.KH. (1995) Nelineynyye dlinnyye volny na poverkhnosti vody i solitony [Nonlinear long waves on the water surface and solitons]. *Journal Advances in Physical Science*, vol. 165, no. 12, pp. 1403–1456.
4. Mei C.C., Black J.L. (1969) Scattering of surface waves by rectangular obstacles in waters of finite depth. *Journal of Fluid Mechanics*, vol. 38, no. 3, pp. 499–511. https://doi.org/10.1017/S0022112069000309
5. Seabra-Santos F. J., Renouard D. P., Temperville A. M. (1987) Numerical and experimental study of the transformation of a solitary wave over a shelf or isolated obstacle. *Journal of Fluid Mechanics*, vol. 176, pp. 117–134. https://doi.org/10.1017/S0022112087000594
6. Losada M.A., Vidal C., Medina R. (1989) Experimental study of the evolution of a solitary wave at an abrupt junction. *Journal of Geophysical Research*, vol. 94, pp. 557–566. https://doi.org/10.1029/JC094iC10p14557
7. Grilli S.T., Losada M.A., Martin F. (1994) Characteristics of solitary wave breaking induced by breakwaters. *Journal of Waterway, Port, Coastal and Ocean Engineering*, vol. 120, no. 1, pp. 75–92. https://doi.org/10.1061/(ASCE)0733-950X(1994)120:1(74)
8. Cooker M.J., Vidal D.H., Dold J.W. (1990) The interaction between a solitary wave and a submerged semicircular cylinder. *Journal of Fluid Mechanics*, vol. 215, pp. 1–22. https://doi.org/10.1017/S002211209000252X

9. Cheng Li G., Ji C., Zhai G. (2020) Solitary wave slamming on an oscillating wave surge converter over varying topography in the presence of collinear currents. *Journal of Physics Fluids*, vol. 32, pp. 047102-1−047102-22. https://doi.org/10.1063/5.0001402
10. Lin P., Liu P.L.F. (1998) A numerical study of breaking waves in the surf zone. *Journal of Fluid Mechanics*, vol. 359, pp. 239–264. https://doi.org/10.1017/S002211209700846X
11. Chang K, Hsu T., Liu P. (2001) Vortex generation and evolution in water waves propagating over a submerged rectangular obstacle. *Journal of Coastal Enineering*, vol. 44, pp. 12–36. https://doi.org/10.1016/S0378-3839(01)00019-9
12. Huang C.-J., Dong C.-M. (2001) On the interaction of a solitary wave and a submerged dike. *Journal of Coastal Enineering*, vol. 43, pp. 265–286. https://doi.org/10.1016/S0378-3839(01)00017-5
13. Lin P.A. (2004) Numerical study of solitary wave interaction with rectangular obstacles. *Journal of Coastal Enineering*, vol. 51. pp. 35–51. https://doi.org/10.1016/j.coastaleng.2003.11.005
14. Baker G.R.,Meiron D., Orszag S.A. (1982) Generalized vortex methods for free-surface flow problems. *Journal of Fluid Mechanics*, vol. 123, pp. 477–501. https://doi.org/10.1017/S0022112082003164
15. Lin M.Y., Huang L.H. (2009) Study of water waves with submerged obstacles using a vortex method with Helmholtz decomposition. *Journal Numerical Methods in Fluids*, vol. 60. pp. 119–148. https://doi.org/10.1002/fld.1873
16. Lin M.Y., Huang L.H. (2010) Vortex shedding from a submerged rectangular obstacle attacked by a solitary wave. *Journal of Fluid Mechanics*, vol. 651, pp. 503–518. https://doi.org/10.1017/S0022112010000145
17. Gorban V.O., Gorban I.M. (2005) Vykhrova struktura potoku pry obtikanni kvadratnoyi pryzmy: chyslova model ta alhorytmy upravlinnya [Vortical flow structure near a square prism: numerical model and algorithms of control]. *Journal of Applied Hydromechanics*, vol. 7, no. 2, pp. 8–26.
18. Gorban I.M. (2015) A numerical study of solitary wave interactions with a bottom step. *Continuous and Distributed Systems II. Springer, Cham*., vol. 30, pp. 369–387. https://doi.org/10.1007/978-3-319-19075-4_22
19. Gorban I.M., Khomenko O.V. (2016) Flow control near a square prism with the help of frontal flat plates. *Advances in Dynamical Systems and Control. Springer, Cham.*, vol. 69. pp. 327–350. https://doi.org/10.1007/978-3-319-40673-2_17
20. Basovsky V.G., Gorban I.M., Khomenko O.V. (2019) Modification of hydrodynamic and acoustic fields generated by a cavity with a fluid suction. *Modern Mathematics and Mechanics. Understanding Complex Systems. Springer, Cham*., pp. 137–158. https://doi.org/10.1007/978-3-319-96755-4_9
21. Lamb H. (1932) *Hydrodynamics*. London: Cambridge University Press.
22. Cottet G.-H., Koumoutsakos P. (2000) *Vortex methods: theory and practice*. London: Cambridge University Press.
23. Molyakov N.M. (1985) Nestatsionarnoye obtekaniye profilya u poverkhnosti razdela zhidkostey [Unsteady flow around a profile under a free surface separating fluids of different densities]. *Proceedings of the Zhukovsky Air Force Engineering Academy*, vol. 1313, pp. 336–347.
24. Israeli M., Orszag S.A. (1981) Approximation of radiation boundary conditions. *Journal of Computer Physic*, vol. 41, pp. 115–135. https://doi.org/10.1016/0021-9991(81)90082-6
25. Seabra-Santos F. J., Renouard D. P., Temperville A. M. (1987) Numerical and experimental study of the transformation of a solitary wave over a shelf or isolated obstacle. *Journal of Fluid Mechanics*, vol. 176, pp. 117–134. https://doi.org/10.1017/S0022112087000594
26. Kotelnikova A.S., Nikishov V.I., Sribnyuk S.M. (2018) Eksperymentalne doslidzhennya vzayemodiyi poverkhnevoyi poodynokoyi khvyli z pidvodnym ustupom [Experimental study of the interaction of a surface solitary wave with a submerged step]. *Hydrodynamics and acoustics*, vol. 1, no. 1, pp. 22−52.
27. Clamond D., Dutykh D. (2013) Fast accurate computation of the fully nonlinear solitary surface gravity waves. *Journal Computers & Fluids*, vol. 84, pp. 35–38. https://doi.org/10.1016/j.compfluid.2013.05.010
28. Madsen O.S., Mei C.C. (1970) The transformation of a solitary wave over an uneven bottom. *Journal of Fluid Mechanics*, vol. 39, № 4, pp. 781–791. https://doi.org/10.1017/S0022112069002461